

Auto-Vocabulary Semantic Segmentation

Osman Ülger^{1*} Maksymilian Kulicki* Yuki Asano¹ Martin R. Oswald¹

University of Amsterdam
{o.ulger,y.m.asano,m.r.oswald}@uva.nl

Abstract. Open-ended image understanding tasks gained significant attention from the research community, particularly with the emergence of Vision-Language Models. Open-Vocabulary Segmentation (OVS) methods are capable of performing semantic segmentation without relying on a fixed vocabulary, and in some cases, they operate without the need for training or fine-tuning. However, OVS methods typically require users to specify the vocabulary based on the task or dataset at hand. In this paper, we introduce *Auto-Vocabulary Semantic Segmentation (AVS)*, advancing open-ended image understanding by eliminating the necessity to predefine object categories for segmentation. Our approach, *AUTOSEG*, presents a framework that autonomously identifies relevant class names using enhanced BLIP embeddings, which are utilized for segmentation afterwards. Given that open-ended object category predictions cannot be directly compared with a fixed ground truth, we develop a Large Language Model-based Auto-Vocabulary Evaluator (LAVE) to efficiently evaluate the automatically generated class names and their corresponding segments. Our method sets new benchmarks on datasets such as PASCAL VOC and Context, ADE20K, and Cityscapes for AVS and showcases competitive performance to OVS methods that require specified class names. All code is publicly available here.

Keywords: Auto-Vocabulary Semantic Segmentation · Open-Vocabulary Semantic Segmentation · Semantic Segmentation

1 Introduction

Semantic segmentation is a computer vision task that involves grouping pixels into coherent regions based on their semantic categories. While notable advancements have been made, existing semantic segmentation models primarily rely on labeled datasets with predefined categories, limiting their ability to handle unknown classes. In contrast, humans possess an open-ended understanding of scenes, recognizing thousands of distinct categories. Recent studies have focused on the development of segmentation models to meet similar capabilities [20, 24], with models that leverage Vision-Language Models (VLMs) as an emerging category [3, 5, 7, 10, 15, 17, 37, 39, 40]. Such VLMs learn rich multi-modal features from large numbers of image-text pairs. Given the scale, training VLMs comes

* Equal contribution.

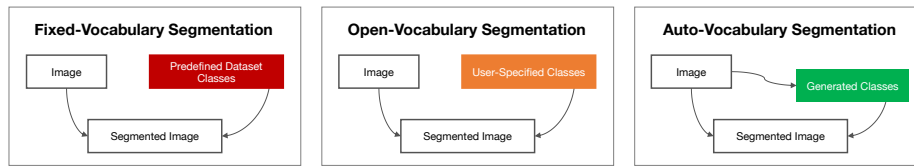


Fig. 1: Different Semantic Segmentation Tasks in Comparison. In traditional Semantic Segmentation, an image is segmented into fixed, predefined dataset classes used during annotation. In Open-Vocabulary Segmentation, the user specifies which object categories (from the open vocabulary) need to be segmented. In Auto-Vocabulary Segmentation, relevant object categories are generated from the image automatically, enabling a true open-ended understanding of scenes without a human in the loop.



Fig. 2: AUTOSEG Exemplary Results. While established segmentation datasets have a fixed set of annotation categories, our method is able to identify and segment object categories beyond the fixed-set ground truth, such as *cub*, *dachshund* or *pagoda*. Images are from the PASCAL VOC [9] and ADE20K [41] datasets.

at an extremely high computational cost. Because of this, it is common to build upon pre-trained VLMs such as CLIP [25] or BLIP [16]. However, applying these VLMs on per-pixel tasks is non-trivial, as they are trained on full images and lack the ability to directly reason over local regions in the image. Previous attempts have employed a two-stage approach where masked regions are fed to the VLMs to produce CLIP embeddings, which are subsequently correlated with text encodings of text prompts to perform classification [7, 17, 38]. Other works directly align per-pixel embeddings with text embeddings retrieved from CLIP [15] based on text prompts provided by the user at test time. While training these models, the text prompts usually correspond to the ground truth class names of the dataset in question. In this paper, we take the capabilities of VLMs one step further and tackle a more challenging task in which the relevant class names are automatically generated. We enable *Auto-Vocabulary Semantic Segmentation (AVS)*, in which the goal is to produce accurate object segmentation and

their pixel-level classifications for **any** class without the need for textual input from the user, predefined class names, additional data, training or fine-tuning.

To tackle this task, we introduce the AUTOSEG framework. Our framework can adapt to any Open-Vocabulary Segmentation (OVS) backbone. We propose BLIP-CLUSTER-CAPTION (BCC) to generate relevant class names, consisting of four simple steps: 1) obtain local BLIP embeddings at different image scales; 2) cluster local BLIP embeddings to identify and separate meaningful semantic areas in the image; 3) caption each clustered embedding and extract nouns from the caption; and 4) pass the resulting nouns to a pre-trained segmentation backbone as class names, thereby essentially creating a self-guided network.

Experimental evaluations on PASCAL VOC [9] and Context [23], ADE20K [41] and Cityscapes [6] showcase the effectiveness of AUTOSEG, achieving state-of-the-art results on AVS and results competitive to OVS methods which are - unlike AUTOSEG- limited by the need for pre-specified class names. It is capable of predicting crisp segmentation masks without having any information a priori about which objects to segment (see Fig. 2). For effective evaluation on public datasets, we furthermore propose a Large Language Model-based Auto-Vocabulary Evaluator (LAVE), tasked with mapping auto-vocabulary predictions to fixed ground truth class names in the dataset. All code will be publicly released to ensure reproducibility and to facilitate further research into AVS.

In summary, our contributions are as follows: **1)** we introduce AUTOSEG, a novel framework to automatically determine and segment relevant classes in an image; **2)** we propose BLIP-CLUSTER-CAPTION, a novel image captioning method capable of generating local and semantically meaningful descriptions from the image obtained from enhanced BLIP embeddings; and **3)** we propose LAVE, a novel evaluation method for auto-vocabulary semantic segmentation which utilizes an LLM. Through qualitative and quantitative analyses, we demonstrate the effectiveness of our framework for Auto-Vocabulary Semantic Segmentation on multiple public datasets.

2 Related Work

Open-Vocabulary Segmentation (OVS). OVS refers to the challenging task of segmenting images based on a list of arbitrary text queries. Contrary to traditional segmentation methods, OVS is not limited to a predefined set of classes. The field of OVS has seen significant advancements through different approaches. Approaching OVS as a zero-shot task, pioneering work by ZS3Net [1] and SP-Net [33] trained custom modules that translate between visual and linguistic embedding spaces and segment by comparing word vectors and local image features. These methods attempt to learn the challenging connection between two very different and independent latent spaces. Consequently, the field of OVS has seen the introduction of methods incorporating Vision-Language Models (VLMs). VLMs pre-train a visual feature encoder with a textual feature encoder on large amounts of image-text pairs, enabling image and text representations to reside in the same feature space. One of such VLMs, Contrastive Language-Image

Pre-training (CLIP) [25], has triggered a wave of segmentation approaches that harness pretrained CLIP embeddings for OVS. LSeg [15] employed the Dense Prediction Transformer to generate per-pixel CLIP embeddings, which are then compared to class embeddings derived from ground-truth segments. More popularly, two-stage approaches such as OpenSeg [10], OPSNet [3], OVSeg [17], ZSSeg [38] and POMP [27] first obtain class-agnostic masks and use CLIP to classify each mask afterwards. Other works, including MaskCLIP [7], FC-CLIP [40], and SAN [37], focus on utilizing intermediate representations from a frozen CLIP encoder. For example, MaskCLIP uses the token features of the ViT-based CLIP encoder and compares local features to class label embeddings instead of pooling them into a global CLIP embedding. The remarkable diversity in the usage of CLIP for OVS extends to works which leverage relationships between image semantics and class labels in CLIP space [5], use CLIP for binary mask prediction [39] or ensure segmentation consistency at different granularity levels using CLIP [31]. Several works have proposed to tackle OVS outside the realm of VLMs using text-to-image diffusion models [11, 34] or custom transformer networks [19, 35, 36, 42]. Most notably, X-Decoder introduces a generalized transformer model capable of performing various vision-language tasks using a single set of parameters. One common and important limitation of the described methods is the need for textual input as a form of guidance by the user. Our work presents a novel framework which enables self-guidance by automatically finding relevant object categories using localized image captioning. Closest and concurrent to our work is the Zero-Guidance Segmentation paradigm [28], in which clustered DINO [2] embeddings are combined with CLIP to achieve zero guidance by the user. Despite the similar setting, there are key differences. While we use the BLIP [16] model for both image clustering and caption generation, they design a complex pipeline consisting of image clustering with DINO, obtaining vision-language embeddings with CLIP and a custom attention-masking module, to then caption these with CLIP-guided GPT-2. This requires converting between three different latent representations throughout the process. In contrast, we achieve superior segmentation quality by enabling self-guidance using any out-of-the-box OVS model.

Image Captioning with Image-Text Embeddings. Image Captioning is the task of describing the content of an image using natural language. A number of approaches have been proposed for the task, including ones utilizing VLMs. Approaches such as CLIP-Cap [22] and CLIP-S [4] utilize CLIP embeddings to guide text generation. More recently, the Large Language and Vision Assistant (LLaVA) was introduced with similar capabilities by connecting the visual encoder of CLIP with a language decoder, as well as training on multimodal instruction-following data [18]. Other approaches rely on BLIP [16], a VLM in which the task of decoding text from image features was one of the tasks of the pretraining process. This enables BLIP to perform image captioning without additional components. Furthermore, the text decoder is guided by local patch embeddings in a way that enables local captioning based on a specific area. This

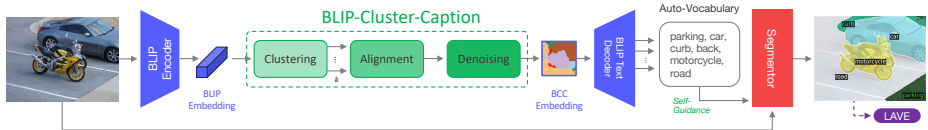


Fig. 3: Method Overview. BLIP encodings are clustered, aligned and denoised before being decoded into nouns. Generated nouns serve as self-guidance to a segmentor, which predicts the final mask. When evaluating (purple), our custom evaluator LAVE processes the output, mapping predicted nouns to the fixed-vocabulary annotations.

unique capability, discovered during the development of our method, emerges organically in BLIP despite being trained solely with image-level captions.

Visual Phrase Grounding. Visual phrase grounding aims to connect different entities mentioned in a caption to corresponding image regions [29]. This task resembles OVS, as it aims to find correspondences between text and image regions. However, predicted areas do not have to precisely outline object boundaries and can be overlapping. Visual grounding has been approached in a self-guided manner, in which heatmaps of regions of the image are generated from image-level CLIP embeddings, which are then captioned by the BLIP encoder [30]. One disadvantage of this approach is that the region determined by CLIP can indicate multiple objects at once, hence multiple objects are captioned for that region, preventing pixel-level class-specific predictions. In our work, BLIP serves both as encoder and decoder, enabling category-specific regions and captioning.

3 Method

This work aims to perform auto-vocabulary semantic segmentation without any additional data, training, finetuning or textual input. To this end, we propose to identify relevant object categories in the image by captioning local image regions at different scales (Sect. 3.1), filtering the generated captions into meaningful semantic descriptions (Sect. 3.2) and using the generated classes names as target categories for a segmentor (Sect. 3.3). An overview is depicted in Fig. 3.

3.1 Local Region Captioning

To identify relevant object categories in the image, we employ Bootstrapped Language Image Pretraining (BLIP) [16]. BLIP is a powerful VLM capable of performing accurate and detailed image captioning. The BLIP image encoder is designed as a Vision Transformer [8], dividing the image into patches and encoding them into embeddings in which image-text representations reside. Subsequently, the set of embeddings is passed through transformer layers to capture contextual information across the image. Finally, all contextualized embeddings are passed to the decoder to generate text descriptions. Though effective in describing salient objects in the image, captioning models like BLIP generally fail to

describe all elements of a scene comprehensively. This is likely due to the descriptions in the training data, which mostly focus on salient foreground objects. This characteristic of VLM pre-training limits its direct application to downstream tasks such as open-ended recognition, in which many objects in the image go unnoticed. As a solution to this limitation, we propose BLIP-CLUSTER-CAPTION (BCC) to enable the BLIP text decoder to consider all encoded areas in the image. BCC clusters the encoded BLIP features into semantically meaningful BLIP feature clusters, which are subsequently enhanced to capture the feature representation of real objects more effectively. Finally, each BLIP feature cluster is fed to the BLIP text decoder separately. This enables generating a description of each semantically meaningful area in the image, resulting in a more comprehensive and accurate description of the image overall.

Clustering. By default, BLIP expects an RGB image $\mathbf{X}_D \in \mathbb{R}^{384 \times 384 \times 3}$. Since common datasets often have images with higher resolution, we additionally process the image at a larger resolution $\mathbf{X}_H \in \mathbb{R}^{512 \times 512 \times 3}$. The multi-resolution set of images $\mathbf{X} = \{\mathbf{X}_D, \mathbf{X}_H\}$ is fed to the BLIP encoder to obtain the set of BLIP patch embeddings $\hat{\mathbf{B}} = \{\hat{\mathbf{B}}^{\mathbf{X}_D}, \hat{\mathbf{B}}^{\mathbf{X}_H}\}$ at the two resolutions:

$$\mathbf{P}^{\mathbf{X}_D} = \{\mathbf{X}_{ij}^D \mid \mathbf{X}_{ij}^D \in \mathbb{R}^{16 \times 16 \times 3}, 1 \leq i, j \leq 24\} \quad (1)$$

$$\mathbf{P}^{\mathbf{X}_H} = \{\mathbf{X}_{ij}^H \mid \mathbf{X}_{ij}^H \in \mathbb{R}^{16 \times 16 \times 3}, 1 \leq i, j \leq 32\} \quad (2)$$

$$\hat{\mathbf{B}}_n^{\mathbf{X}_R} = T(f_{\text{MLP}}(\mathbf{P}_n^{\mathbf{X}_R})) \oplus \mathbf{z}_n^{\mathbf{X}_R}, \quad \forall n \in \{1, 2, \dots, N\} \quad (3)$$

where $\mathbf{P}^{\mathbf{X}_D} \in \mathbb{R}^{576 \times 16 \times 16 \times 3}$ and $\mathbf{P}^{\mathbf{X}_H} \in \mathbb{R}^{1024 \times 16 \times 16 \times 3}$ denote the set of patches in resolutions D and H respectively, $f_{\text{MLP}}(\cdot)$ represents a shared fully connected Multi-Layer Perceptron (MLP) and T is a Transformer encoder, consisting of L alternating layers of Multi-Head Self-Attention (MHA) and an MLP, sequentially propagated with the function composition operator \circ :

$$T_l(X) = X + \text{MHA}(\text{LAYERNORM}(X, X, X)) \quad (4)$$

$$\hat{T}_l(X) = T_l(X) + f_{\text{MLP}}(\text{LAYERNORM}(T_l(X))) \quad (5)$$

$$T(X) = (\hat{T}_{L-1} \circ \hat{T}_{L-2} \circ \dots \circ \hat{T}_0)(X). \quad (6)$$

In Eq. (3), we additionally concatenate a sinusoidal positional encoding¹ [32] $\mathbf{z}_i \in \mathbb{R}^{256}$ to each patch i to encode spatial information, where N is the total number of patches for each resolution R . Next, we cluster the patches in $\hat{\mathbf{B}}$ for each resolution R using k -means clustering [21]:

$$C_k^R = \underset{C}{\text{argmin}} \sum_{i=1}^N \min_{\mu_j \in C} \|\hat{\mathbf{B}}_i^{\mathbf{X}_R} - \mu_j\|^2 \quad (7)$$

where C_k is the set of k clusters and μ_i are the cluster centroids. Running the clustering procedure with a 2 to 8 range for k on two different image resolutions results in 14 different cluster assignments.

¹ Obtained with the positional-encodings Python library.

Cross-clustering Consistency. Each run of k -means clustering labels its clusters independently from others, yielding a correspondence mismatch between clusters across runs. To resolve this, we relabel the cluster indices to a common reference frame with the following steps:

1. Select C with the most clusters after k -means as a reference set S . As some clusters end up empty during the k -means iterations, this is not always the set with highest initial k . The reference set determines the indices used for all other sets of clusters \mathcal{C} , each with its number of clusters denoted by $|C_i|$:

$$S = \operatorname{argmax}_{C_i \in \mathcal{C}} |C_i| \quad (8)$$

2. Sets of clusters are aligned to the reference set using Hungarian matching [14]. We calculate pairwise Intersection over Union (IoU) between the clusters from S and C . Then, each cluster from C is assigned a new index, matching the cluster with the highest IoU from S :

$$\begin{aligned} &\text{For each cluster } c_j \in C, \quad j \in \{1, \dots, |C|\} : \\ &\text{Assign index } i \text{ to } c_j \text{ where } i = \operatorname{argmax}_{i \in \{1, \dots, |S|\}} \operatorname{IoU}(c_j, s_i) \end{aligned} \quad (9)$$

3. With the labeled sets of clusters, a probability distribution over the clusters is assigned to each image patch. For a given patch p , let $\mathbf{L}(p) = \{\mathbf{L}_1(p), \mathbf{L}_2(p), \dots, \mathbf{L}_m(p)\}$ be the set of labels assigned to p by the m different sets of clusters. The probability $P(n|p)$ of p being assigned to a particular cluster n is defined as the relative frequency of n among labels $\mathbf{L}(p)$:

$$P(n|p) = \frac{\sum_{i=1}^m \mathbb{1}}{m}, \text{ with } \mathbb{1} = \begin{cases} 1, & \text{if } \mathbf{L}_i(p) = n \\ 0, & \text{else} \end{cases} \quad (10)$$

The predictions of a single k -means predictor tend to contain high levels of noise, likely due to the high dimensionality of the embeddings. Our method can be seen as an ensemble, reducing the variance present in each individual predictor. The areas that are consistently clustered together by various predictors are likely to be semantically connected. In addition, our method enables for a flexible number of output clusters. Some of the initial clusters can disappear if they are not well-supported by multiple predictors. This property is highly desired due to the variety of input images and the number of objects in them.

Cluster Denoising. To further improve the locality and semantic meaningfulness of clustered feature representations, we apply a Conditional Random Field (CRF)² [13] and majority filter. CRF is a discriminative statistical method that is used to denoise predictions based on local interactions between them. In our case, the predictions are a 2D grid of cluster assignment probabilities of the image patches. Our implementation is specifically tailored for refining 2D segmentation map, using a mean field approximation with a convolutional approach to iteratively adjust the probability distributions of each image patch’s cluster indices.

² We use the crfseg Python library.

Key to this process is the use of a Gaussian filter in the pairwise potentials, which ensures spatial smoothness and consistency in the segmentation.

The application of the CRF yields embeddings which are less noisy and more cohesive than the original aligned k -means result. To address remaining noise in the embeddings, a neighborhood majority filter is applied as a final step. For each image patch, we consider the set of patches $\mathcal{N}(i, j)$ in its square neighborhood: $\mathcal{N}(i, j) = \{(i + \delta_i, j + \delta_j) \mid \delta_i, \delta_j \in \{-1, 0, 1\}\}$. The mode value from the cluster indices in that neighborhood is calculated and assigned as the new index of the central patch:

$$\text{mode}(\mathcal{N}(i, j)) = \underset{k \in K}{\operatorname{argmax}} \sum_{m \in \mathcal{N}(i, j)} \mathbb{1}_{\text{index}(m)=k} \quad (11)$$

This step is applied recursively until convergence or 8 times at most. In the supplementary material, we visualize the effect of each step on the embeddings.

Captioning. The next step involves turning clustered, denoised and enhanced BLIP embeddings into text. The BLIP text decoder is a Transformer architecture capable of processing unordered sets of embeddings of arbitrary size. We leverage this feature and feed flattened subsets of patch embeddings, each corresponding to a cluster, to the BLIP text decoder. Spatial information is preserved due to the presence of positional embeddings added in the clustering step. With this technique, our method essentially infers semantic categories captured by clusters and represented by BLIP embeddings. To the best of our knowledge, we are the first to use the text decoder in this manner, enabling local captioning for which it was never specifically trained. The caption generation is stochastic, with different object namings appearing in the captions depending on initialization. To obtain a rich, unbiased and diverse set of object names, we regenerate captions with each embedding multiple times in caption generation *cycles*.

3.2 Caption Filtering

The captions generated by the BLIP text decoder are sentences in natural language. For our task, we are only interested in the class names present in each sentence. To obtain these, we filter the sentence down to relevant class names using noun extraction. Captions are parsed using the spaCy model³ to provide a part-of-speech label for each word in the caption. Words labeled as nouns are kept and converted into their singular form through lemmatization. We collect all nouns generated by different clusters and cycles into one noun set and remove any duplicates, as well as nouns which do not appear in the WordNet dictionary.

3.3 Self-Guidance

The output of the clustered BLIP embeddings (see Sect. 3.1) is a 32x32 grid with cluster index assignments. Each element of the grid corresponds to an

³ www.spacy.io/models/en#en_core_web_sm

image patch from the original image, which enables us to create segmentation masks - defined as a union of areas covered by image patches with the same index - essentially for free. For example, Fig. 3 shows the clustered output as a 2-dimensional mask, which succeeds in masking relevant objects to a certain extent. However, the segmentation outputs are constrained to a 32x32 resolution of the BLIP encoder. Upsampling yields unsatisfactory results, since objects appear oversegmented and boundaries remain unsharp. Another challenge is to associate each mask with one class name. In this cluster representation, masked areas are described with sentences rather than single nouns. When such a sentence contains multiple nouns, it is not trivial which noun to select as the predicted class name for that mask. To perform effective and accurate auto-vocabulary semantic segmentation, we leverage BCC’s strength in generating an elaborate set of relevant class names and use this as textual guidance for a pre-trained OVS model capable of producing high-resolution outputs. BCC is model-agnostic, therefore any kind of OVS model that expects an image and a set of class labels can be combined with our method. We focus on X-Decoder [42], which is a popular and well-performing OVS model.

3.4 Custom Open-Vocabulary Evaluator

As discussed in Sect. 2, previous works in OVS have mainly focused on a setting where the target class names are provided by the user. Hence, evaluation is possible by having access to the ground truth of those target class names during evaluation. However, in scenarios where the target class names are discovered rather than pre-specified, as in our framework, there may be a lack of direct alignment between the semantics of these categories and the classes used in the annotations. In zero-guidance segmentation [28], the authors have proposed to align class names based on the cosine-similarity in the latent space of Sentence-BERT [26] or CLIP [25]. In our initial experiments, this yielded unsatisfactory results where, even in obvious cases, the open-vocabulary classes were linked to the incorrect class (*e.g.* taxi to road instead of car). This led to a decline in performance as measured by segmentation metrics, yet the method showed promising results from a qualitative perspective. Relations between two class names can be complex, such as synonymy, hyponymy, hypernymy, meronymy or holonymy, which exceed the capabilities of a cosine-similarity criterium in the respective latent spaces. As a possible solution, we propose an **LLM-based Auto-Vocabulary Evaluator (LAVE)**. Specifically, we employ the Llama 2 7B Large Language model⁴ with the task of mapping predicted auto-vocabulary categories to target categories in the dataset. First, AUTOSEG returns a segmentation mask with classes from an auto-vocabulary generated by BCC. Second, LAVE collects all uniquely predicted auto-vocabulary categories in the output and builds a mapper from each predicted category to the most relevant or similar target category. Thirdly, all pixel values in the segmentation mask belonging to each

⁴ www.huggingface.co/meta-llama/Llama-2-7b

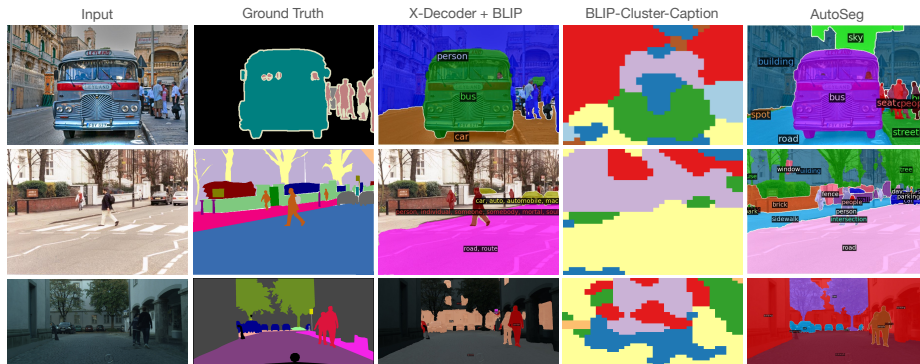


Fig. 4: Segmentation with VLMs. Example outputs on PASCAL VOC/Context (top), ADE20K (middle) and Cityscapes (bottom) by feeding plain BLIP embeddings to X-Decoder, directly using BCC embeddings as masks and AUTOSEG. Notably, our method segments images in the most comprehensive and accurate manner.

class are updated respectively according to the mapper. Finally, the mean Intersection over Union (mIoU) is computed with the updated segmentation mask. Pseudocode and prompts for LAVE are provided in the supplementary material.

4 Experiments

4.1 Experimental Setup

We evaluate our method on three popular semantic segmentation validation datasets: PASCAL VOC [9] and Context [23], ADE20K [41] and Cityscapes [6] with 20, 459, 847 and 20 classes respectively. These datasets cover a wide range of difficulty and class diversity. For example, ADE20K is challenging with its many and infrequently appearing classes, while Cityscapes contains many object instances per image. We list dataset statistics in Tab. 2.

Evaluation. For quantitative comparison with previous works, we use mIoU as the main metric. As mentioned in Sec. 3.4, class predictions in the segmentation mask are mapped using LAVE before the mIoU is computed. Furthermore, to study the class-agnostic segmentation performance of different VLMs, we report class-agnostic mean Intersection over Union (cmIoU). The computation of cmIoU involves the following steps. First, pairwise IoU values, denoted as $\text{IoU}(g_i, p_j)$ are calculated between all ground-truth segments g_i and predicted segments p_j from a given image. Each g_i segment is matched with the predicted segment p_{\max_i} that yields the highest IoU value: $p_{\max_i} = \arg \max_j \text{IoU}(g_i, p_j)$. The cmIoU is then determined by calculating the arithmetic mean of these highest IoU values across the dataset, which can be formulated as $\text{cmIoU} = \frac{1}{N} \sum_{i=1}^N \text{IoU}_{\max_i}$ where N is the total number of ground-truth segments in the dataset.

Table 1: Ablations on Segmentation with VLMs. Class-agnostic mIoU values for different variants of our method. AUTOSEG, which combines BCC with X-Decoder segmentation, achieves the best performance on all four datasets.

Approach	VOC [9]	PC-459 [23]	ADE20K [41]	Cityscapes [6]
X-DECODER [42] + BLIP [16]	38.0	35.3	26.7	29.2
BLIP-CLUSTER-CAPTION	16.3	16.3	11.3	0.85
AUTOSEG	71.8	47.7	29.2	35.8

Implementation details. For our experiments, we use the BLIP model built with ViT-Large backbone and finetuned for image captioning on the COCO dataset in combination with the Focal-L variant of X-Decoder. For both models, we use publicly available pretrained weights and do not perform any additional finetuning. Parameter tuning is performed for the clustering and captioning modules. Parameters of the clustering include image scales encoded by BLIP (384×384 and 512×512), the k values of k -means clustering (2 to 8), the parameters of Gaussian smoothing in the CRF (smoothness weight of 6 and smoothness θ of 0.8), the number of iterations of majority filtering (8) and the feature dimension size of the positional embeddings (256). As for text generation, we opted for nucleus sampling with a minimum length of 4 tokens and maximum of 25, top P value of 1 and repetition penalty of 100 to ensure as many unique nouns as possible. These parameters were determined using Bayesian optimization on VOC with the goal of maximizing the mIoU.

4.2 Ablations

To investigate the performance of different configurations of our framework, we present two ablation studies. The first ablation study investigates different methods of using a VLM to obtain segmentation masks. In the second, we examine the effect of different amounts of captioning cycles.

Segmentation with Vision Language Models. A VLM can be leveraged in different ways to obtain segmentation masks. In this ablation study, we study the benefit of using an auto-vocabulary generated with BCC for segmentation as in AUTOSEG. In order to do so, we compare our method against a scenario where plain BLIP embeddings are used for captioning instead of enhanced ones. Furthermore, we also evaluate the extent to which BCC embedding outputs themselves can be used directly as segmentation masks (see Sect. 3.3) after up-sampling. Due to the difficulty of establishing correspondence between BCC clusters and ground-truth labels, we evaluate the segmentation quality using cmIoU. Quantitative results are reported in Tab. 1. On all four datasets, AUTOSEG performs most effectively. Comparing X-DECODER + BLIP to AUTOSEG qualitatively, one can observe that the former suffers from false positives and false negatives simultaneously, which in turn serves as an explanation for the performance gap in cmIoU. For example, in PASCAL, it incorrectly masks the area around the bus at the cost of segmenting people. In ADE20K and Cityscapes, it

Table 2: Ablations on Captioning Cycles. The optimal number of captioning cycles varies per dataset. On Cityscapes, which has images in the highest resolution, most instances (\bar{I}) and classes on average (\bar{C}), AUTOSEG benefits from 25 cycles, while between 1 and 15 captioning cycles for datasets with fewer instances per image suffices.

Dataset	\bar{I}	\bar{C}	C	Number of Captioning Cycles					
				1	5	10	15	20	25
PASCAL VOC [9]	3.5	3.5	20	85.3	84.4	87.1	85.7	83.3	83.3
PASCAL Context [23]	18.9	6.2	459	10.1	9.7	11.2	11.7	9.6	10.8
ADE20K [41]	19.5	10.5	847	5.9	5.8	5.1	5.2	5.1	5.6
Cityscapes [6]	34.3	17	20	28.2	28.1	28.4	28.3	27.9	29.5

ignores large parts of the area which could appear to BLIP as insignificant. Our framework ensures that smaller, less salient objects are effectively captioned. As expected, intermediate masks of BCC do not segment objects sufficiently accurate due to the low resolution of the embedding space. Interestingly, it is still capable of segmenting global areas linked to certain objects in PASCAL and ADE20K, while failing completely for Cityscapes, likely due to the higher instance count and higher resolution of images.

Captioning Cycles. A key aspect of our model is its capability to iteratively repeat the captioning process within BCC, enabling it to generate a more exhaustive collection of nouns which accurately describe the scene. This approach proves especially beneficial in instances where objects are initially overlooked or described with less precise semantic terms. To assess the impact, we explore the effects of single versus multiple captioning iterations — 5, 10, 15, 20, or 25 times — using the mIoU metric. The findings, presented in Tab. 2, reveal that the optimal number of captioning cycles varies significantly with the dataset in question. Specifically, we observe that for the Cityscapes dataset, characterized by its high average number of instances and unique classes per image (denoted as \bar{I} and \bar{C} in Tab. 2, respectively), a greater number of cycles yields the most benefit. For datasets with a lower average number of instances and unique classes per image, like VOC or ADE20K, fewer captioning cycles are required for BCC to identify all relevant class names. As anticipated, our model requires a greater number of captioning cycles for the Context dataset, which, despite featuring images identical to those in VOC, includes annotations for an additional 439 object categories. Remarkably, AUTOSEG successfully handles ADE20K, the dataset with the largest number of unique classes in our experiments, using merely a single captioning cycle. This outcome underscores our model’s ability in efficiently addressing complex datasets which resemble an open-ended setting.

4.3 Quantitative Analysis

We compare our method against existing OVS methods that require class names to be given, as well as with Zero-Guidance Segmentation (referred to as ZeroSeg [28]). Tab. 3 shows the results. Without any specification of class names

Table 3: Quantitative Results (mIoU). AUTOSEG performs competitive with existing OVS methods which require class names, while achieving superior performance on the zero label setting. Results with dashes are not published and unavailable.

Method	Auto-Classes	VOC [9]	PC-459 [23]	ADE20K [41]	Cityscapes [6]
LSEG [15]	✗	47.4	-	-	-
OVSEGMENTOR [36]	✗	53.8	20.4	-	-
SIMSEG [39]	✗	57.4	26.2	-	-
OVDIFF [11]	✗	69.0	31.4	-	-
OPENSEG [10]	✗	72.2	45.9	8.8	-
OVSEG [17]	✗	94.5	55.7	9.0	-
ODISE [34]	✗	82.7	57.3	11.0	-
SAN [37]	✗	94.6	57.7	12.4	-
CAT-SEG [5]	✗	97.2	62.0	13.3	-
ZSSEG [38]	✗	83.5	47.7	7.0	34.5
X-DECODER [42]	✗	96.2	65.1	6.4	50.8
FC-CLIP [40]	✗	95.4	58.4	14.8	56.2
ZEROSEG [28]	✓	20.1	11.4	-	-
AUTOSEG (Ours)	✓	87.1	11.7	5.9	29.5

through user input, AUTOSEG achieves 86%, 18%, 40% and 52% of the best performing OVS methods on VOC, Context, ADE20K and Cityscapes respectively. The difference in performance can be attributed to AUTOSEG needing to identify the subjects for segmentation independently, while OVS methods are explicitly instructed on the specific objects to segment. Remarkably, however, AUTOSEG is able to remarkably surpass the performance many OVS methods on VOC, such as OVDIFF [11], OPENSEG [10] or ODISE [34], without any access to the ground truth class names. While still leaving room for improvement, our model compares competitively with OVS methods on ADE20K and Cityscapes, two very challenging datasets either high in number of unique classes or instances. Comparing to ZeroSeg, AUTOSEG achieves superior performance on VOC (87.1 over 20.1 mIoU) and Context (11.7 over 11.4 mIoU). Furthermore, we set a new state-of-the-art on ADE20K and Cityscapes under the auto-class generation task setting. This outcome underscores the efficacy of our method in dealing with complex scenes that have an open-ended nature, such as ADE20K with its large number of rare classes. While other models have to decide between 847 possibilities, AUTOSEG suggests a smaller yet more relevant set of class names. Our method deals well with high numbers of instances and can successfully identify various non-salient objects. A comparison with the findings from Tab. 2 reveals that while BCC struggles with providing high-quality masks on its own, it is able to identify the accurate target classes, which can subsequently be segmented with precision. Additional experiments are provided in the supplementary material, in which we generate class names with other image captioning methods and compare the segmentation performance of such vocabularies. Overall, our results demonstrate that the integration of BCC and OVS harnesses the strengths of both, leading to enhanced open-ended recognition capabilities.



Fig. 5: Qualitative Results. AUTOSEG shows remarkable capability to identify out-of-vocabulary categories, such as *hawk* or *coke*, and segment them accurately across different datasets. The first two rows highlight results on from PASCAL VOC/Context, while the bottom two rows are from ADE20K and Cityscapes respectively.

4.4 Qualitative Analysis

Fig. 5 displays qualitative results on the four datasets, where AUTOSEG demonstrates its capability to comprehensively detect and accurately segment relevant object categories within the images. Remarkably, it predicts segmentation masks for specific class names such as *hawk*, *piano*, *wildflower*, *officer* or *coke* - all categories not listed in the annotations of their respective datasets. Moreover, in certain instances, AUTOSEG successfully captures additional contextual details, such as *graduation* or *exercise*, illustrating the model’s capabilities at recognizing objects in scenes in a genuinely open-ended manner. Additional results, as well as failure cases, are available in the supplementary material.

5 Conclusion

In this work we introduced AUTOSEG, a novel method which leverages a vision-language model to automatically identify relevant target classes and segment them - a task we termed Auto-Vocabulary Semantic Segmentation. Additionally, we proposed LAVE, a new evaluation method which employs an LLM to map

open-ended class names to ground-truth labels. AUTOSEG demonstrates remarkable open-ended recognition capabilities, achieving state-of-the-art performance on the zero label setting, while being competitive with open-vocabulary segmentation models which require ground-truth label specification.

Acknowledgements. This work was supported by TomTom, the University of Amsterdam and the allowance of Top consortia for Knowledge and Innovation (TKIs) from the Netherlands Ministry of Economic Affairs and Climate Policy.

Supplementary Material

Appendix A. LLM-based Auto-Vocabulary Evaluator

This appendix provides more insight into the pseudocode and text prompts of the *LLM Mapper* which maps auto-vocabulary classes to the fixed-vocabulary classes present in the annotations of each respective dataset. The LLM Mapper is a key component of our **LLM-based Auto-Vocabulary Evaluation Metric (LAVE)** and enables the evaluation of predicted auto-vocabulary classes on public benchmarks. By doing so, we enable comparison with open-vocabulary methods, such as in Tab. 3, which predict a fixed-vocabulary for evaluation.

LLM Mapper Pseudocode

The LLM Mapper is tasked with creating a mapping dictionary which maps from auto-vocabulary classes to fixed-vocabulary classes. The resulting mapping dictionary can be used during inference to map pixel-level class predictions belonging to an automatically generated - out-of-vocabulary- class to fixed-vocabulary class indices. In Alg. 1, we detail the procedure to create the mapping dictionary.

LLM Mapping Prompts

The `generateDialogs()` function in the LLM Mapper takes a prompt template as one of its inputs. This prompt template is dependent on the dataset and is used to generate dialogs to query the LLM with. For PASCAL VOC and Cityscapes, we explicitly specify the list of categories given its short length with 20 classes each. For PASCAL Context and ADE20K, with its 459 and 849 classes respectively, we rely on the LLM’s knowledge of the datasets. Explicitly naming each object class from these datasets causes the LLM to run into memory issues when queried with long dialogues. We specify the prompt templates for each respective dataset as follows:

PASCAL VOC and Cityscapes

To which class in the list `<dataset>` is `<name>` exclusively most similar to? If `<name>` is not similar to any class in the list or if the term describes stuff instead of things, answer with ‘background’. Reply in single quotation marks with the class name that is part of the list `<dataset>` and do not link it to any other class name which is not part of the given list or ‘background’.

where `<noun>` is the noun to map to the vocabulary and `<dataset>` is the list of classes of PASCAL VOC or Cityscapes.

Table 4: Experiments with Alternative Class Generation Baselines (mIoU). Experiments with alternative methods to generate classes showcase that AUTOSEG is favorable for AVS across all three datasets, with larger performance gaps on VOC and Cityscapes with a smaller vocabulary size.

Approach	VOC [9]	PC-459 [23]	Cityscapes [6]
SAM + BLIP + X-DECODER	41.1	11.3	27.4
LLAVA + X-DECODER	56.7	11.4	23.4
AUTOSEG	87.1	11.7	29.5

PASCAL Context and ADE20K

To which class in the <dataset> dataset is <name> exclusively most similar to? If <name> is not similar to any class in <dataset> or if the term describes stuff instead of things, answer with ‘background’. Reply in single quotation marks with the class name that is part of <dataset> and do not link it to any other class name which is not part of the given list or ‘background’.

where <noun> is the noun to map to the vocabulary and <dataset> is either ‘PASCAL-Context 459’ or ‘ADE20K’.

Appendix B. Alternative Class Generation Baselines

In Tab. 4, we provide additional comparisons with alternative methods to generate class names from images. In particular, we compare against an altered version of BLIP to caption the image at an object instance level with segments retrieved from the Segment Anything Model (SAM) [12]. We use segment everything prompting, *i.e.* the model’s object proposal generation functionality. Furthermore, we compare against Large Language and Vision Assistant (LLAVA) [18], generating classes with the prompt ‘Please name all the elements present in the image as a list of nouns’. We compare the mIoU performance on VOC, Context and Cityscapes and find that AUTOSEG performs favorably over other approaches that are adjusted to segment with automatically generated classes. The performance gap is especially high for datasets with a small vocabulary, such as VOC and Cityscapes, possibly indicating that AUTOSEG is better able in generating classes that are relevant for prediction while the other methods generate redundant classes which become false positive predictions. In contrast to both SAM and LLAVA, AUTOSEG has an additional benefit of being independent of prompting. For this reason, our method does not require prompt engineering in order to obtain class names effective for accurate segmentation.

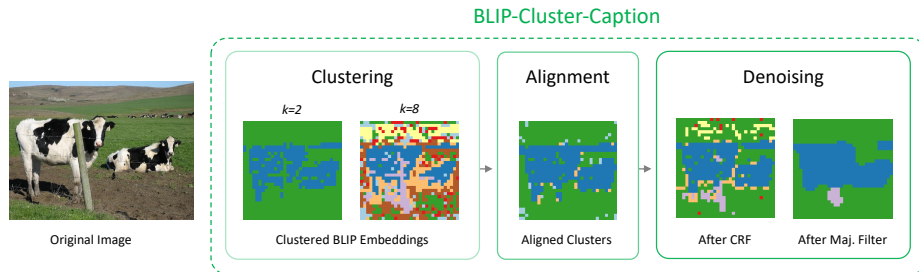


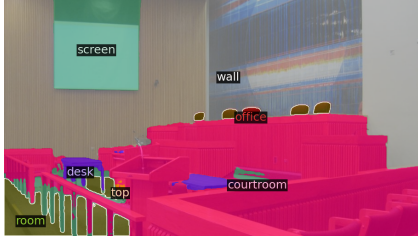
Fig. 6: Visualization of Intermediate BCC Outputs. Intermediate BCC outputs show how BLIP embeddings are enhanced with each individual step of Clustering, Alignment or Denoising.

Appendix C. Visualization of Embeddings in BCC

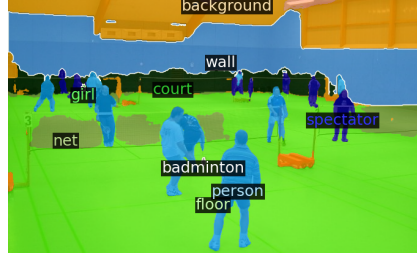
In Fig. 6, we visualize intermediate 32×32 outputs of BCC to better understand what each individual step of Clustering, Alignment or Denoising achieves. Firstly, Fig. 6 reveals that clustering BLIP embeddings results grouping pixels into semantic areas. With $k = 2$, the image is divided an area which includes the cows (in blue) and another for everything else (green), while for $k = 8$, various other objects - such as the pole in purple - get included. At this stage, the embeddings appear noisy and inconsistent across all k , which is why the combination of all clusters is so important. The alignment output shows that certain objects from a higher k embeddings are now included in those of lower k embeddings, *i.e.* the aligned embedding captures a more extensive list of objects present in the image. Finally, to further reduce the noise in the embedding, we apply CRF and a majority filter. We see that the final embedding consists of three unique semantic areas, which are eventually fed to the BLIP text decoder for captioning.

Appendix D. Additional Qualitative Results

In Fig. 7, 8 and 9, we provide additional qualitative results of AUTOSEG and discuss observed capabilities or limitations in the caption of each figure.



(a) **Success Case.** AUTOSEG can infer detailed class names, such as *courtroom*, which is non-existent in the extensive vocabulary of the dataset.



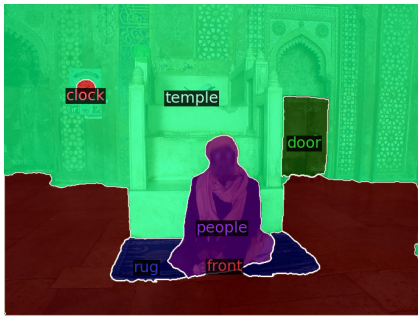
(b) **Success Case.** The class *badminton* is not part of ADE20K. Despite taking up a very small area in the image, AUTOSEG is still capable of segmenting it.



(c) **Success Case.** AUTOSEG displays advanced scene understanding capabilities. Here, it recognizes the out-of-vocabulary class *reflection*, which requires the model to reason about other auto-generated classes and structural properties in the image.



(d) **Success Case.** The rare and out-of-vocabulary class name *dinosaur* is generated automatically and segmented by AUTOSEG.. This is another example of the method's efficacy on long-tailed classes.



(e) **Failure Case.** AUTOSEG's occasionally struggles with indoor scenes from specific buildings, such as a mosque in this image. Our model mistakenly regards it a temple.



(f) **Failure Case.** Here, AUTOSEG predicts the zebra rug as a *zebra* as a result of noun parsing. After BCC has generated captions from the image, both *zebra* and *rug* get parsed into individual nouns. When fed to the segmentor, *zebra* eventually ends up being predicted as the more relevant class name.

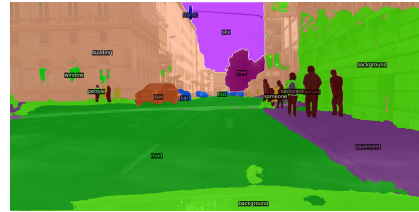
Fig. 7: Additional Qualitative Results on ADE20K.



(a) **Success Case.** Despite the visual similarities between a *moped* and *motorcycle*, AUTOSEG correctly considers both and segments them accurately. A supervised model would fail to generalize to *moped*, as it is out of Cityscapes’ vocabulary.



(c) **Success Case.** AUTOSEG is able to provide class names which can be crucial for real-life scenarios, such as *hazard* in this example. The standard 20 classes in Cityscapes do not account for such objects descriptions.



(b) **Success Case.** While annotations in Cityscapes consider all car types to be equal, AUTOSEG often generates more specific descriptions, such as the *SUV* in this image.

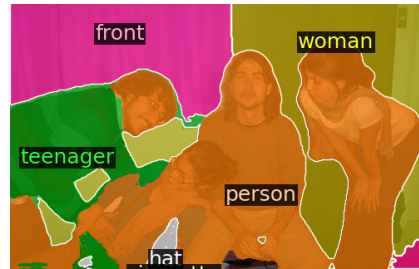


(d) **Failure Case.** Occasionally, generated class names, such as *street*, dominate the search space of the segmentor and cause it to attend more on that class. This may result in oversegmentation and other class names, such as *car*, to be ignored.

Fig. 8: Additional Qualitative Results on Cityscapes.



(a) **Success Case.** AUTOSEG is able to accurately classify and segment classes not present in the dataset, such as the *ox*.



(b) **Failure Case.** Generated nouns are occasionally hyponyms or hypernyms of each other, causing the classes to “compete” for the final segmentation. Future work could possibly address this by checking for such relations between nouns and correcting for them.

Fig. 9: Additional Qualitative Results on PASCAL.

Algorithm 1 LLM Mapper

Require: *nouns*, *dataset_vocabulary*, *llm_batch_size*, *prompt_template*, **LLM**

```

all_responses, map_dict, skipped  $\leftarrow$  initialize()
for batch in split(nouns, llm_batch_size) do
  dialogs  $\leftarrow$  generateDialogs(batch, prompt_template)
  batch_responses  $\leftarrow$  LLM(dialogs)
  store(all_responses, (batch_responses, batch))
end for

for (batch_response, batch) in all_responses do
  for (response, noun) in (batch_response, batch) do
    answer  $\leftarrow$  parseResponse(response)
    common  $\leftarrow$  intersect(answer, dataset_vocabulary)
    updateDict(map_dict, noun, common)
    updateSkipped(skipped, noun, common)
  end for
end for

for key in map_dict do
  if key is in vocabulary then
    map_dict[key]  $\leftarrow$  key
  end if
  if key is in skipped then
    skipped  $\leftarrow$  removeItem(skipped, key)
  end if
end for

for skipped_key in skipped do
  map_dict[skipped_key]  $\leftarrow$  "background"
end for

return map_dict

```

References

1. Bucher, M., VU, T.H., Cord, M., Pérez, P.: Zero-shot semantic segmentation. In: Wallach, H., Larochelle, H., Beygelzimer, A., d'Alché-Buc, F., Fox, E., Garnett, R. (eds.) *NeurIPS* (2019)
2. Caron, M., Touvron, H., Misra, I., Jégou, H., Mairal, J., Bojanowski, P., Joulin, A.: Emerging properties in self-supervised vision transformers. In: *ICCV* (2021)
3. Chen, X., Li, S., Lim, S.N., Torralba, A., Zhao, H.: Open-vocabulary panoptic segmentation with embedding modulation. In: *ICCV* (2023)
4. Cho, J., Yoon, S., Kale, A., Derroncourt, F., Bui, T., Bansal, M.: Fine-grained image captioning with clip reward. *arXiv preprint arXiv:2205.13115* (2023)
5. Cho, S., Shin, H., Hong, S., An, S., Lee, S., Arnab, A., Seo, P.H., Kim, S.: Cat-seg: Cost aggregation for open-vocabulary semantic segmentation. *arXiv preprint arXiv:2303.11797* (2023)
6. Cordts, M., Omran, M., Ramos, S., Rehfeld, T., Enzweiler, M., Benenson, R., Franke, U., Roth, S., Schiele, B.: The cityscapes dataset for semantic urban scene understanding. In: *CVPR* (2016)
7. Dong, X., Bao, J., Zheng, Y., Zhang, T., Chen, D., Yang, H., Zeng, M., Zhang, W., Yuan, L., Chen, D., Wen, F., Yu, N.: Maskclip: Masked self-distillation advances contrastive language-image pretraining. *arXiv preprint arXiv:2208.12262* (2023)
8. Dosovitskiy, A., Beyer, L., Kolesnikov, A., Weissenborn, D., Zhai, X., Unterthiner, T., Dehghani, M., Minderer, M., Heigold, G., Gelly, S., et al.: An image is worth 16x16 words: Transformers for image recognition at scale. *arXiv preprint arXiv:2010.11929* (2020)
9. Everingham, M., Gool, L.V., Williams, C.K.I., Winn, J.M., Zisserman, A.: The pascal visual object classes (voc) challenge. *IJCV* (2010)
10. Ghiasi, G., Gu, X., Cui, Y., Lin, T.: Scaling open-vocabulary image segmentation with image-level labels. *ECCV* (2022)
11. Karazija, L., Laina, I., Vedaldi, A., Rupprecht, C.: Diffusion Models for Zero-Shot Open-Vocabulary Segmentation. *arXiv preprint arXiv:2306.09316* (2023)
12. Kirillov, A., Mintun, E., Ravi, N., Mao, H., Rolland, C., Gustafson, L., Xiao, T., Whitehead, S., Berg, A.C., Lo, W.Y., Dollar, P., Girshick, R.: Segment anything. In: *ICCV* (2023)
13. Krähenbühl, P., Koltun, V.: Efficient inference in fully connected crfs with gaussian edge potentials. *Advances in neural information processing systems* **24** (2011)
14. Kuhn, H.W.: The hungarian method for the assignment problem. *Naval Research Logistics Quarterly* **2**(1-2), 83–97 (1955)
15. Li, B., Weinberger, K.Q., Belongie, S.J., Koltun, V., Ranftl, R.: Language-driven semantic segmentation. *ICLR* (2022)
16. Li, J., Li, D., Xiong, C., Hoi, S.: Blip: Bootstrapping language-image pre-training for unified vision-language understanding and generation. In: *ICML* (2022)
17. Liang, F., Wu, B., Dai, X., Li, K., Zhao, Y., Zhang, H., Zhang, P., Vajda, P., Marculescu, D.: Open-vocabulary semantic segmentation with mask-adapted clip. *CVPR* (2023)
18. Liu, H., Li, C., Wu, Q., Lee, Y.J.: Visual instruction tuning. In: *NeurIPS* (2023)
19. Liu, Q., Wen, Y., Han, J., Xu, C., Xu, H., Liang, X.: Open-world semantic segmentation via contrasting and clustering vision-language embedding. In: *ECCV* (2022)
20. Ma, C., Yang, Y., Wang, Y., Zhang, Y., Xie, W.: Open-vocabulary semantic segmentation with frozen vision-language models. In: *BMVC* (2022)

21. MacQueen, J., et al.: Some methods for classification and analysis of multivariate observations. In: Proceedings of the fifth Berkeley symposium on mathematical statistics and probability. pp. 281–297 (1967)
22. Mokady, R., Hertz, A., Bermano, A.H.: Clipcap: Clip prefix for image captioning. arXiv preprint arXiv:2111.09734 (2021)
23. Mottaghi, R., Chen, X., Liu, X., Cho, N.G., Lee, S.W., Fidler, S., Urtasun, R., Yuille, A.: The role of context for object detection and semantic segmentation in the wild. In: Proceedings of the IEEE conference on computer vision and pattern recognition. pp. 891–898 (2014)
24. Pandey, P., Chasmai, M., Natarajan, M., Lall, B.: A language-guided benchmark for weakly supervised open vocabulary semantic segmentation. arXiv preprint arXiv:2302.14163 (2023)
25. Radford, A., Kim, J.W., Hallacy, C., Ramesh, A., Goh, G., Agarwal, S., Sastry, G., Askell, A., Mishkin, P., Clark, J., Krueger, G., Sutskever, I.: Learning transferable visual models from natural language supervision. In: ICML (2021)
26. Reimers, N., Gurevych, I.: Sentence-bert: Sentence embeddings using siamese bert-networks. EMNLP (2019)
27. Ren, S., Zhang, A., Zhu, Y., Zhang, S., Zheng, S., Li, M., Smola, A., Sun, X.: Prompt pre-training with twenty-thousand classes for open-vocabulary visual recognition. In: NeurIPS (2023)
28. Rewatbowornwong, P., Chatthee, N., Chuangsuwanich, E., Suwajanakorn, S.: Zero-guidance segmentation using zero segment labels. In: ICCV (2023)
29. Rohrbach, A., Rohrbach, M., Hu, R., Darrell, T., Schiele, B.: Grounding of textual phrases in images by reconstruction. In: ECCV (2016)
30. Shaharabany, T., Tewel, Y., Wolf, L.: What is where by looking: Weakly-supervised open-world phrase-grounding without text inputs. NeurIPS (2022)
31. Sun, P., Chen, S., Zhu, C., Xiao, F., Luo, P., Xie, S., Yan, Z.: Going denser with open-vocabulary part segmentation. In: ICCV (2023)
32. Vaswani, A., Shazeer, N., Parmar, N., Uszkoreit, J., Jones, L., Gomez, A.N., Kaiser, Ł., Polosukhin, I.: Attention is all you need. In: NeurIPS (2017)
33. Xian, Y., Choudhury, S., He, Y., Schiele, B., Akata, Z.: Semantic projection network for zero- and few-label semantic segmentation. In: CVPR (2019)
34. Xu, J., Liu, S., Vahdat, A., Byeon, W., Wang, X., De Mello, S.: Open-Vocabulary Panoptic Segmentation with Text-to-Image Diffusion Models. ICCV (2023)
35. Xu, J., Mello, S.D., Liu, S., Byeon, W., Breuel, T., Kautz, J., Wang, X.: Groupvit: Semantic segmentation emerges from text supervision. CVPR (2022)
36. Xu, J., Hou, J., Zhang, Y., Feng, R., Wang, Y., Qiao, Y., Xie, W.: Learning open-vocabulary semantic segmentation models from natural language supervision. In: CVPR (2023)
37. Xu, M., Zhang, Z., Wei, F., Hu, H., Bai, X.: Side adapter network for open-vocabulary semantic segmentation. In: CVPR (2023)
38. Xu, M., Zhang, Z., Wei, F., Lin, Y., Cao, Y., Hu, H., , Bai, X.: A simple baseline for open vocabulary semantic segmentation with pre-trained vision-language model. ECCV (2022)
39. Yi, M., Cui, Q., Wu, H., Yang, C., Yoshie, O., Lu, H.: A simple framework for text-supervised semantic segmentation. In: CVPR (2023)
40. Yu, Q., He, J., Deng, X., Shen, X., Chen, L.C.: Convolutions die hard: Open-vocabulary segmentation with single frozen convolutional clip. In: NeurIPS (2023)
41. Zhou, B., Zhao, H., Puig, X., Fidler, S., Barriuso, A., Torralba, A.: Scene parsing through ade20k dataset. In: CVPR (2017)

42. Zou, X., Dou, Z.Y., Yang, J., Gan, Z., Li, L., Li, C., Dai, X., Behl, H., Wang, J., Yuan, L., Peng, N., Wang, L., Lee, Y.J., Gao, J.: Generalized decoding for pixel, image, and language. CVPR (2023)